Microsc. Microanal. Microstruct. **4** (1993) 575–594 DECEMBER **1993**, PAGE 575

Classification
Physics Abstracts
61.14 — 61.16B — 61.66

Study of the iron-nitrogen phases by electron microdiffraction and convergent beam electron diffraction

Jean-Paul Morniroli, Olivier Richard and Jacques Foct

Laboratoire de Métallurgie Physique, URA CNRS 234, Bât. C6, Université de Lille I, 59655 Villeneuve d'Ascq Cedex, France

(Received October 25, 1993; accepted February 08, 1994)

Résumé. — On montre comment la microdiffraction électronique associée à la diffraction électronique en faisceau convergent a permis d'identifier sans ambiguïté le groupe spatial des phases γ, γ' et ε du diagramme Fe-N. La méthode utilisée implique l'identification préalable, à partir de clichés de microdiffraction, d'un symbole partiel d'extinction en concordance avec quelques groupes spatiaux. L'identification définitive du groupe spatial est ensuite réalisée au moyen de la méthode "multifaisceaux" de Tanaka ou à partir de l'observation de l'intensité des faisceaux diffractés sur les clichés de microdiffraction. On explique comment surmonter les difficultés expérimentales liées à la petite taille des cristaux, à la texture des échantillons observés et à la non observation des zones de Laue d'ordres supérieurs sur la plupart des clichés de diffraction.

Abstract. — It is shown how electron microdiffraction connected with convergent beam electron diffraction can be used to identify unambiguously the space group of the γ, γ' and ε iron nitrides. The method involves the identification, from microdiffraction patterns, of a partial extinction symbol in agreement with a few possible space groups. The actual space group is then identified by means of the Tanaka "multibeam" method or from observation of the intensity of the diffracted beams on microdiffraction patterns. It is explained how to overcome the experimental difficulties connected with the small crystal size, the texture of the specimen and the absence of HOLZ reflections on most diffraction patterns.

1. Introduction.

Due to their high saturation magnetization iron nitrides and Fe-N solid solutions constitute a promising class of materials for applications in electronics. Manufacturing of these materials and understanding of the role of microstructure on magnetic properties are the matter of important research and development studies. In some cases the influence of nitrogen ordering has been shown to be critical. The aim of this paper is to show that beside classical diffraction studies and spectroscopic results, electron microdiffraction and convergent beam electron diffraction are suitable tools for studying their microstructure.

The identification and characterization of phases by means of Convergent Beam Electron Diffraction (CBED) is now well established. CBED allows the identification of the point group of a crystal by a method described by Buxton *et al.* [1] or by a "multibeam" method proposed by Tanaka [2]. The space group can also be inferred from observation of Gjonnes and Moodie lines of dynamical absence present on CBED patterns [3].

It has been shown recently that microdiffraction patterns obtained with a nearly parallel electron beam and a small spot size can also be used, in connection with CBED patterns or independently, to identify phases [4-9].

In connection with CBED, microdiffraction allows the identification of a few possible space groups, which usually belong to different point groups. The actual space group is then determined from identification of the point group by CBED. To choose among the possible point groups, the simplest CBED experiments can be performed. For example, CBED patterns which only exhibit 2D features, are often valuable and their use constitutes an important experimental simplification.

Microdiffraction can also be used independently [4]. This is particularly useful when a specimen gives too poor a CBED pattern to be of any help in the identification of the point group. This occurs frequently with small particles or with faulted specimens. Even in these difficult cases, good microdiffraction patterns are often obtained. They can be used to deduce a few possible space groups and eventually the point group can be obtained from observation of the diffracted beams intensity.

In order to test the validity of microdiffraction with actual specimens, three phases present in the Fe-N phase diagram, namely the γ, γ' and ε phases, were studied. Several experimental difficulties were encountered. Most of them were connected with the small crystal sizes, the magnetism and the strong texture of the specimens. Other experimental difficulties were connected with the ordering of the nitrogen atoms and with the absence of High Order Laue Zone (HOLZ) reflections on most microdiffraction patterns.

2. Microdiffraction patterns.

The information present on microdiffraction patterns allows one to identify the crystal system, the orientation of the crystal with respect to the electron beam (i.e. the zone axis), the Bravais lattice and the glide planes of the structure [4].

2.1 IDENTIFICATION OF THE CRYSTAL SYSTEM AND OF THE ZONE AXIS. — First, the crystal system is identified from observation of the "net" symmetry of microdiffraction patterns. This is the symmetry of the pattern which only takes into account the position of the reflections on the pattern (the intensity is not considered). The "net" symmetry of the ZOLZ (Zero Order Laue Zone) and/or of the whole pattern (WP) constituted of the ZOLZ and HOLZ (High Order Laue Zone) reflections may be considered.

The identification is made by searching the microdiffraction pattern which exhibits the highest "net" symmetry. The crystal system is then deduced by means of table I. Once the crystal system is identified, the zone axis of any pattern can be determined from its "net" symmetry by means of table II.

Note: For all the crystal systems, except for the cubic and the tetragonal ones, the identification of the crystal system requires observation of the WP "net" symmetries. This implies that HOLZ reflections, or at least FOLZ reflections, are present on the microdiffraction pattern. Very often

Table I. — *Identification of the crystal system from the whole pattern "net" symmetry. (Reproduced from Morniroli and Steeds, 1992, with permission of the publisher.)*

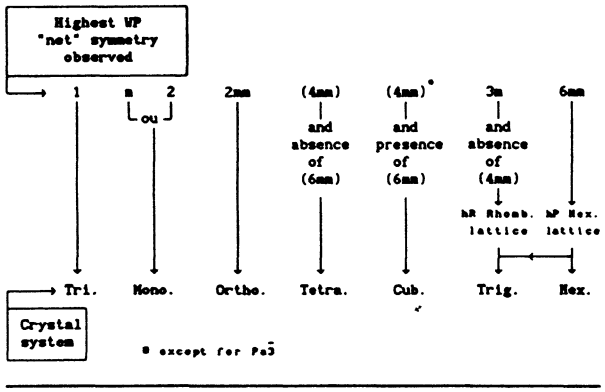

Table II. — *Identification of the zone axis from the "net" symmetry. (Reproduced from Morniroli and Steeds, 1992, with permission of the publisher.)*

"Net" symmetry								
Whole pattern	ZOLZ							
6mm	(6mm)							[0001]
3m	(6mm)					⟨111⟩	[0001]	
4mm	(4mm)				[001]	⟨001⟩		
2mm	(2mm)			[001]	⟨100⟩	⟨110⟩		⟨11$\bar{2}$0⟩
				[010]	⟨110⟩	⟨001⟩ for Pa$\bar{3}$		⟨1$\bar{1}$00⟩
				[100]				
m	(2mm)		[u0w]	[u0w]	⟨u0w⟩	⟨uv0⟩	[$u\bar{u}$0w]	[uvt0]
				[0$v$$w$]	[uv0]	⟨uuw⟩		[$u\bar{u}$0w]
				[uv0]	[uuw]			[uu$\bar{2}$u$\bar{w}$]
2	(2)		[010]				⟨11$\bar{2}$0⟩	
1	(2)	[uvw]	[uvw]	[uvw]	[uvw]	[uvw]	[$uvtw$]	[$uvtw$]
Crystal system		Tri.	Mono.	Ortho.	Tetra.	Cubic	hR rhombohedral Bravais lattice Trigonal	hP hexagonal Bravais lattice Hexagonal

these reflections are not observed, due to the following reasons:
- the zone axis parameter $p_{[uvw]}$ is too small, giving a FOLZ radius too great to be observed,
- the maximum visible diffraction angle of the electron microscope is too small,
- the intensity of the FOLZ reflections is too weak.

To solve these problems, the microscope voltage can be decreased so as to reduce the Ewald

sphere radius or the specimen cooled so as to enhance the diffracted beam intensity. A better solution, used in this study, consists of tilting the specimen along the ZOLZ mirrors until more or less large sections of the HOLZ appear. In this way, the FOLZ and HOLZ reflection nets can be reconstructed and the WP symmetry elements identified.

2.2 IDENTIFICATION OF THE BRAVAIS LATTICE. — Forbidden reflections associated with the non-primitive Bravais lattices cannot appear by multiple diffraction and, as a result, produce typical shifts between the ZOLZ and the FOLZ reflection nets for the specific zone axes given in table III. This feature is clearly revealed by observing the presence or the absence of FOLZ reflections along the "net" mirrors [5, 6].

Table III. — *Zone axes used to characterize the Bravais lattice and the glide planes. (Reproduced from Morniroli and Steeds, 1992, with permission of the publisher.)*

Crystal system	Mono. unique axis *b*	Ortho.	Tetragonal	Cubic	Hexagonal	Trigonal	
Zones axes required for identification of the Bravais lattice	[010] or [0$\bar{1}$0]	[100] or [010] or [001]	[001]	⟨001⟩ and ⟨110⟩ for cI and cF	P only	P or R only	
Zone axes required for simultaneous identifications of the Bravais lattice and glide planes	[010] or [0$\bar{1}$0]	[100] and [010] and [001]	[001] and ⟨100⟩ and ⟨110⟩	⟨001⟩ and ⟨110⟩	⟨11$\bar{2}$0⟩ and ⟨1$\bar{1}$00⟩	Rhombohedral Bravais lattice ⟨11$\bar{2}$0⟩	Hexagonal Bravais lattice ⟨11$\bar{2}$0⟩ and ⟨1$\bar{1}$00⟩

2.3 IDENTIFICATION OF THE GLIDE PLANES. — Glide planes produce kinematical forbidden reflections which usually appear by multiple diffraction on most microdiffraction patterns, except for on the particular zone axes which are exactly perpendicular to the glide planes. In these cases the forbidden reflections are actually absent and can be clearly distinguished from the allowed reflections, since all the possible multiple diffraction paths are cancelled. As a result, a typical periodicity difference between the ZOLZ and the FOLZ reflection nets is observed on the corresponding microdiffraction patterns. This difference is easily revealed and characterized by drawing in the ZOLZ and in the FOLZ, the smallest rectangle or square with sides parallel to the "net" mirrors [7, 8, 10].

2.4 IDENTIFICATION OF THE PARTIAL EXTINCTION SYMBOL. — As shown in table III, for most crystal systems, identification of the Bravais lattices and of the glide planes requires observation of the same zone axes. In order to facilitate this simultaneous identification, we have drawn, for each of the crystal systems, the theoretical microdiffraction patterns for all possible Bravais lattices

and for all possible glide planes. In addition to a direct identification made by simple comparison between experimental and theoretical patterns, each theoretical pattern gives an individual partial extinction symbol as introduced by Buerger for X-ray diffraction experiments [11]. The symbol is only partial since the theoretical patterns do not take into account the presence of screw axes. Depending on the crystal system, addition of one, two or three individual symbols coming from one, two or three required zone axes leads to the partial extinction symbol. The resulting symbol is in agreement with a few possible space groups listed in table 3.2 of the International Tables for Crystallography [12].

This identification of a few possible space groups from a limited number of zone axis microdiffraction patterns in terms of tables and diagrams constitutes a formal scheme. In order to obtain the whole extinction symbol the scheme can be completed by including screw axis detection by means of the specific experiments described in reference [4]. Any additional information present on microdiffraction pattern can also be used to supplement the analysis.

3. Sample preparation and conventions.

The methods mentioned above are applied to the study of the γ, γ' and ε phases belonging to the iron-nitrogen diagram.

The specimens are elaborated by gas flow nitriding (H_2/NH_3) between 500 °C and 700 °C of thin pure iron sheets.

The γ and γ' specimens are electropolished in a solution containing 10% perchloric acid and 90% acetic acid (in volume) at 15 °C under a 50 V operating voltage.

The ε phase which is very brittle is thinned by ion milling with argon ions accelerated to 5 kV.

The thin foils are observed with a PHILIPS CM30 electron microscope working at 300 kV. The spot size is in the range 20 nm to 500 nm.

The notation and conventions used in this paper, are the same as those given in reference [4].

The ZOLZ mirrors and symmetries are noted between parentheses in order to distinguish them from the WP ones.

The "ideal" mirrors and symmetries, which take into account the position and the intensity of the reflections on the pattern, are underlined in order to distinguish them from the "net" ones.

A diffraction pattern with a 2 mm symmetry, contains two perpendicular mirrors, m_1 and m_2. The mirror noted m_1 is the one that is parallel to the larger side of the smallest rectangle which can be drawn in the FOLZ.

A diffraction pattern with a 4 mm symmetry, contains two sets of perpendicular mirrors. The first set is composed of the mirrors noted m_1 and m_2, which are parallel to the sides of the smallest square drawn in the FOLZ. The mirrors belonging to the second set are noted m_1' and m_2'.

A diffraction pattern with 6 mm symmetry, contains two sets of three mirrors at 30° from each other. The three mirrors which cross the nearest ZOLZ reflections are noted m_1, m_2, m_3. The three other mirrors are noted m_1', m_2', m_3'.

4. Experimental results.

4.1 STUDY OF THE γ PHASE. — The highest ZOLZ "net" symmetry displayed by a microdiffraction pattern from the γ phase is (4 mm) (Fig. 1a). Since the first order Laue zone is not present in this pattern, it is necessary, in order to identify the whole pattern "net" symmetry, to tilt the

specimen along the ZOLZ mirrors (m_1) and (m_1') until more or less large sections of the FOLZ reflection net appear. The corresponding patterns, given in figures 1b and c, allow one to reconstruct the FOLZ and then to clearly reveal the presence of WP "net" mirrors m_1 and m_1'. As a result, the WP "net" symmetry is 4 mm and, according to tables I and II, the crystal system is either cubic or tetragonal and the zone axis is $< 001 >$. No pattern with (6 mm) ZOLZ "net" symmetry has ever been observed. This fact would seem to indicate that the crystal system is tetragonal. Nevertheless, since the specimen exhibits a strong texture, some caution should be taken prior to making a final conclusion.

The pattern given in figure 2a has (2 mm) ZOLZ "net" symmetry. Once again the 2 mm WP "net" symmetry is obtained by tilting the specimen along the ZOLZ mirrors (m_1) and (m_2) (Figs. 2b and c). As indicated in table II, a pattern with (2 mm), 2 mm "net" symmetries is in agreement with the $< 100 >$ or $< 110 >$ zone axes if the crystal system is tetragonal or with the $< 110 >$ zone axis if the system is cubic. In the experimental pattern of figure 2a, the angle between the mirror m_2 and the diagonal d across the rectangle drawn in the ZOLZ with sides parallel to the mirrors (m_1) and (m_2), equals 54.5°. This is very close to the theoretical value 54.7°, which is typical of the $\{111\}$ and $\{002\}$ interplanar angle for the cubic system. This fact removes the ambiguity between the two possible crystal systems and proves that the system is indeed cubic.

For the cubic crystal system, the simultaneous identification of the Bravais lattice and the glide planes requires examination of the $< 001 >$ and $< 110 >$ zone axis patterns (see Tab. III).

For the $< 001 >$ ZAP, reconstruction of the FOLZ reflection net from patterns 1b and c allows one to draw in the FOLZ, the smallest square and then to define, using the conventions given above, the two sets of WP "net" mirrors m_1, m_2 and m_1', m_2'. The smallest square with sides parallel to m_1, m_2 is also drawn in the ZOLZ. One notices that the ZOLZ and FOLZ squares are identical, indicating that there is no ZOLZ/FOLZ periodicity difference and therefore no glide plane. In addition, FOLZ reflections are present on mirrors m_1', m_2' but absent on mirrors m_1, m_2. Taking these features into account, a direct comparison can be made with the theoretical patterns of figure 1d. A perfect agreement is observed with the theoretical pattern corresponding to the individual partial extinction symbol F-.. or I-.. .

The same approach is used for the $< 110 >$ ZAP. The FOLZ reflection net is reconstructed from figures 2b and c, and the same smallest centered rectangles with sides parallel to m_1, m_2 are drawn in the FOLZ and in the ZOLZ. FOLZ reflections are present on both mirrors m_1 and m_2. According to the theoretical patterns of figure 2d, the individual partial extinction symbol, is F..- .

Note: Only the even layers of the reciprocal lattice exist for the $< 110 >$ ZAP in the case of a face centered cubic lattice. As a result, it is not the first order Laue zone that is present on patterns 2b and c, but the second one, called SOLZ (Second Order Laue Zone).

From the $< 001 >$ and $< 110 >$ ZAPs, the Bravais lattice I is discarded and the F-.- partial extinction symbol is inferred by adding the two previous symbols. According to table 3.2 in reference [12], this is in agreement with the six space groups belonging to the five point groups given in the following table:

point group	23	$m\bar{3}$	432	$\bar{4}3m$	$m\bar{3}m$
space group	F23	$Fm\bar{3}$	F432 $F4_132$	$F\bar{4}3m$	$Fm\bar{3}m$

The point group can be identified by using the Tanaka "multibeam" method [2]. From exami-

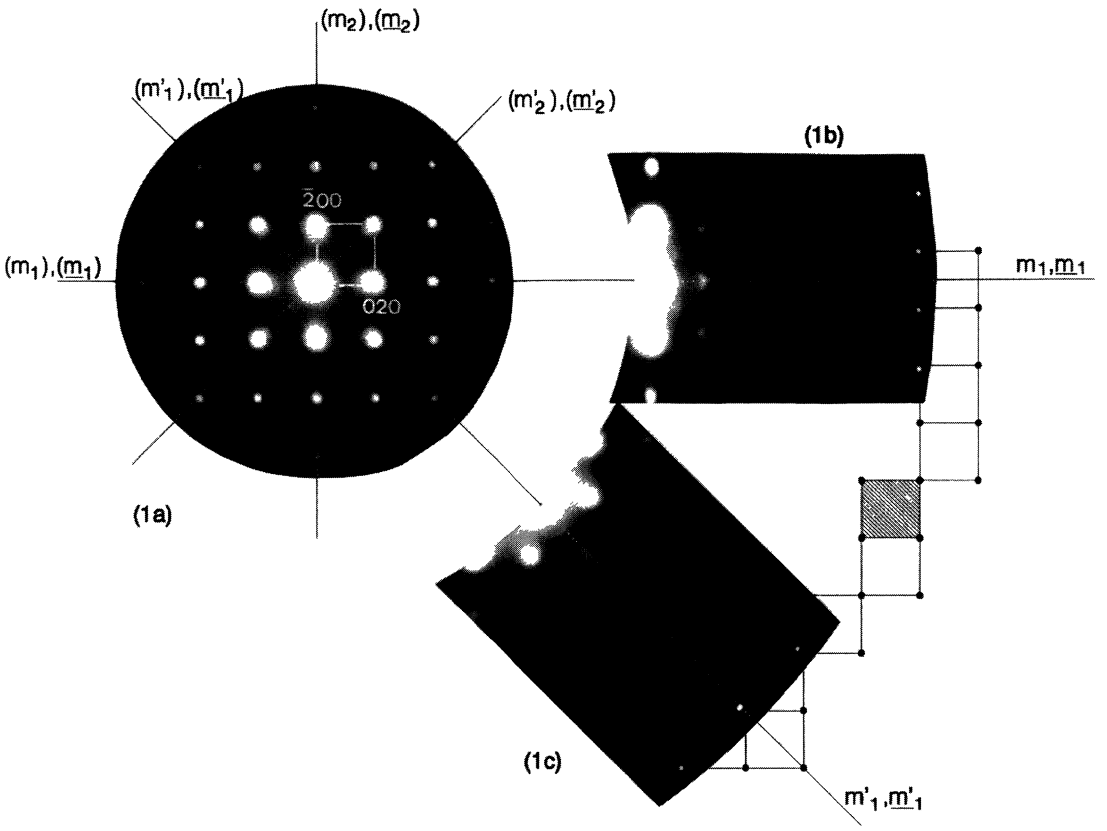

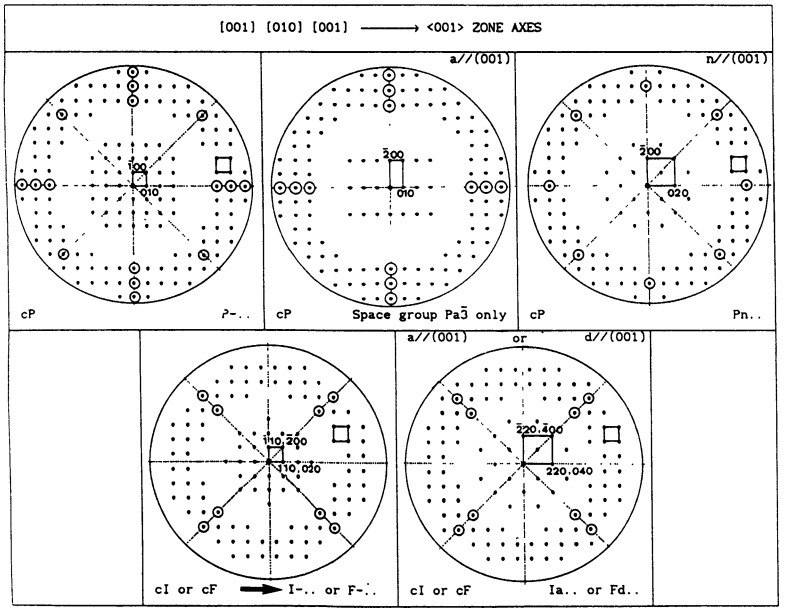

Fig. 1. — γ Fe-N phase. a) b) c) < 100 > zone axis pattern. d) Theoretical < 100 > ZAPs for the cubic system. (Reproduced from Morniroli and Steeds, 1992, with permission of the publisher.)

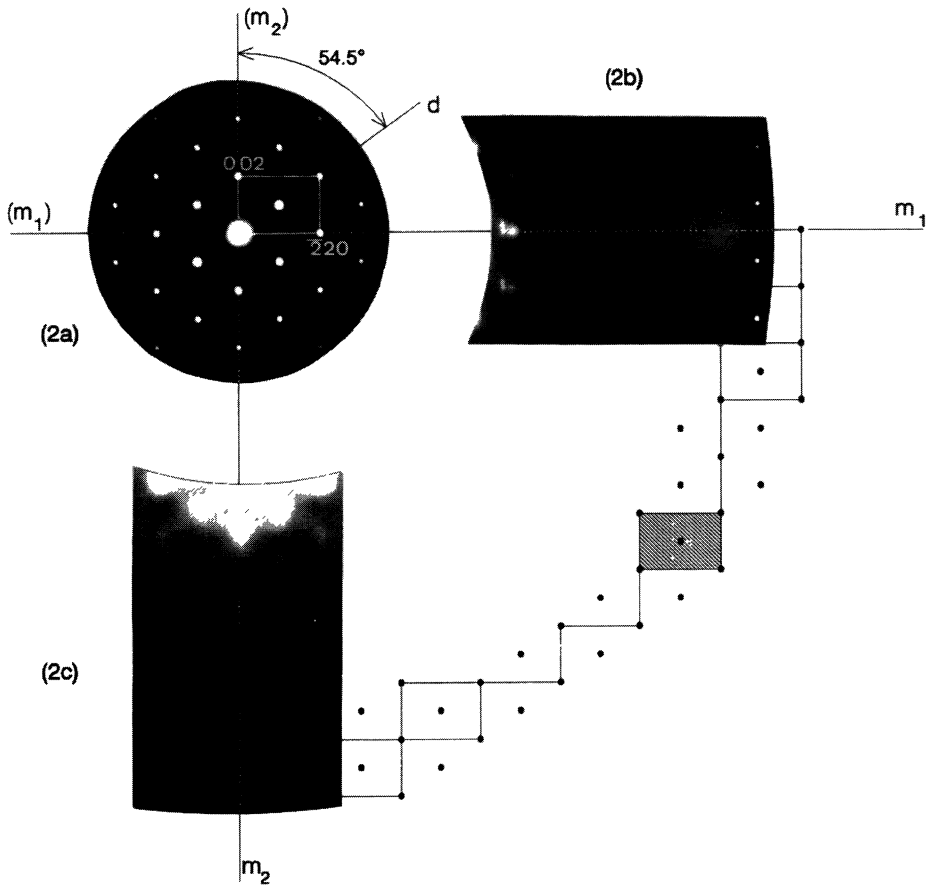

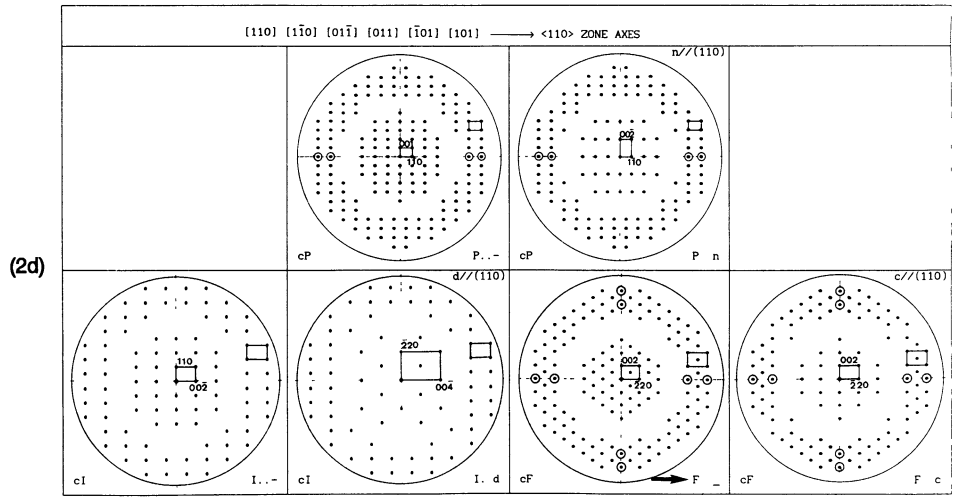

(2d)

Fig. 2. — γ Fe-N phase. a) b) c) < 110 > zone axis pattern. d) Theoretical < 110 > ZAPs for the cubic system. (Reproduced from Morniroli and Steeds, 1992, with permission of the publisher.)

nation of table 4 in reference [1], the simplest CBED experiments to perform can be planned. For example, observation of the $< uuw >$ ZAP is a good choice here since 3/5 point groups can be identified from CBED patterns which only exhibit 2D information, as indicated in the following table:

	<uuw> zone axes	
	diffraction group	
point group	3D	2D
$m\bar{3}m$	$2_R mm_R$	$2mm1_R$
$4\bar{3}m$	m	$m1_R$
432	m_R	$m1_R$
$m\bar{3}$	2_R	21_R
23	1	1_R

The $< 332 >$ zone axis multibeam pattern given in figure 3a only contains 2D information inside the discs and reveals the presence of a 2 fold axis in the $1\bar{3}3$ reflection and of a mirror in the $2\bar{2}0$ and $\bar{1}\bar{1}3$ reflections. This is in perfect agreement with the $2mm1_R$ projection diffraction group (Fig. 3b) [2].

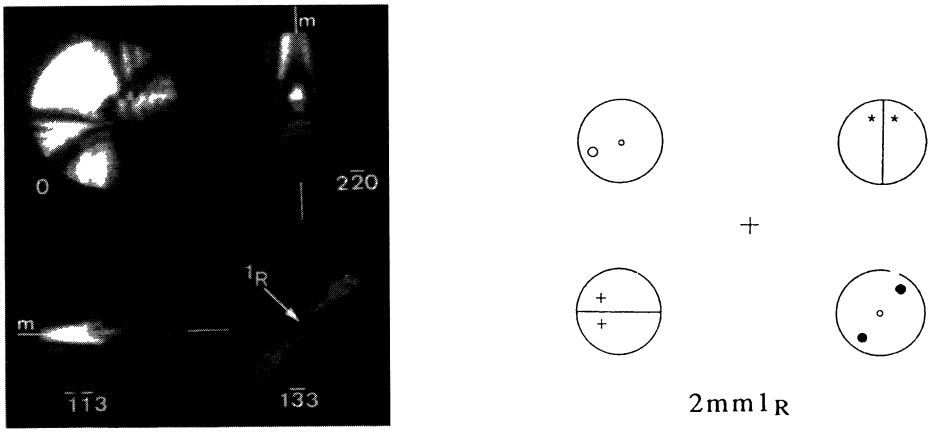

Fig. 3. — γ Fe-N phase. a) $< 332 >$ zone axis Tanaka "multibeam" pattern. b) Symmetry elements for the $2mm1_R$ diffraction group.

Since this diffraction group only corresponds to the $m\bar{3}m$ point group, the space group for the γ phase is therefore $Fm\bar{3}m$.

An alternative method of identifying the point group consists of observing the whole pattern "ideal" symmetry [4], that is, the symmetry that takes into account both the position and the

intensity of the reflections. For the cubic system (Tab. IV), the ZAP to observe is < 001 >. Since its "ideal" symmetry is (4mm), 4mm (Figs. 1a, b, c), the corresponding point and space groups are $m\bar{3}m$ and $Fm\bar{3}m$ respectively.

Table IV. — *Identification of the point group from the "ideal" symmetry for the cubic system. (Reproduced from Morniroli and Steeds, 1992, with permission of the publisher.)*

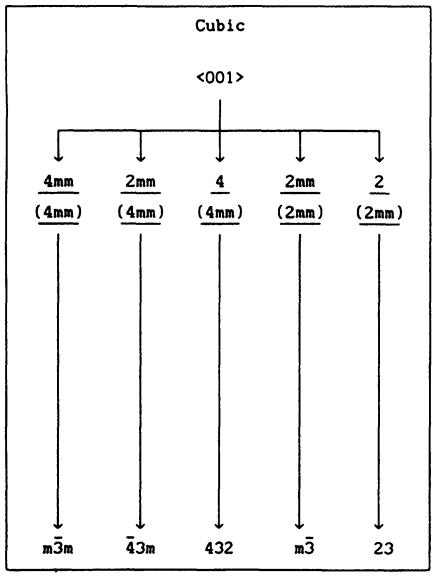

4.2 STUDY OF THE γ' PHASE. — Most of the microdiffraction patterns from the γ' phase exhibit both strong and weak reflections. The strong ones are fundamental reflections and the weak ones are superlattice reflections which are due to the ordering of the nitrogen atoms in interstitial sites of the lattice. It is imperative that the superlattice reflections are taken into account in the characterization of the structure. The fundamental reflections are not sufficient since they only give information about the iron basal lattice.

The highest "net" symmetry observed for the γ' phase is (4 mm), 4 mm (Figs. 4a, b and c). As in the previous case, the 4 mm WP "net" symmetry is obtained by tilting the specimen along the mirrors present in the ZOLZ. According to tables I and II, the crystal system is either cubic or tetragonal and the corresponding zone axis is < 001 >. The (6 mm) ZOLZ "net" symmetry is not observed, but once again this absence may be due to the strong texture of the specimen.

The pattern given in figures 5a, b, c, exhibits (2 mm), 2 mm "net" symmetries. A 54.5° angle, typical of the cubic system, is also measured on this pattern between (m_2) and d, proving that the crystal system is cubic.

Identification of the Bravais lattice and the glide planes requires observation of both the < 001 > and the < 110 > ZAPs (Tab. III).

On the < 001 > ZAP (Figs. 4a, b, c), the same non-centered squares with sides parallel to m_1 and m_2 can be drawn in the ZOLZ and in the FOLZ, indicating that there is no periodicity difference between the ZOLZ and the FOLZ reflection nets. FOLZ reflections are present

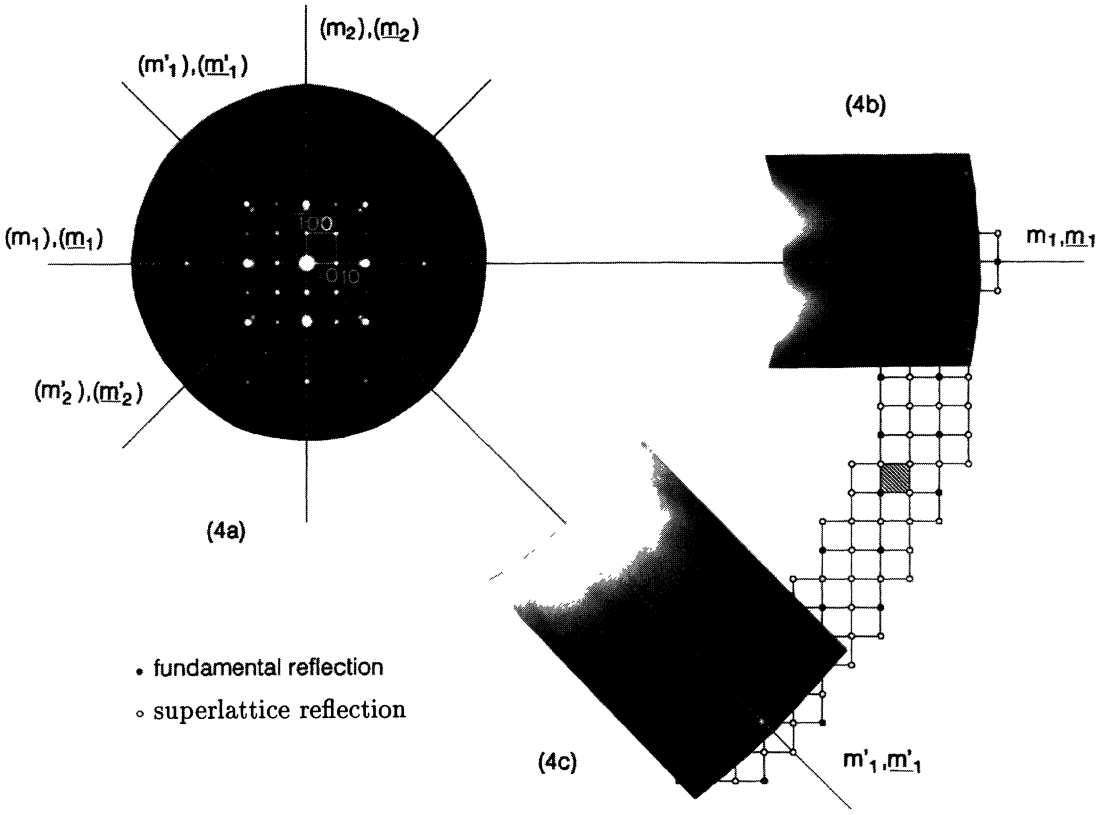

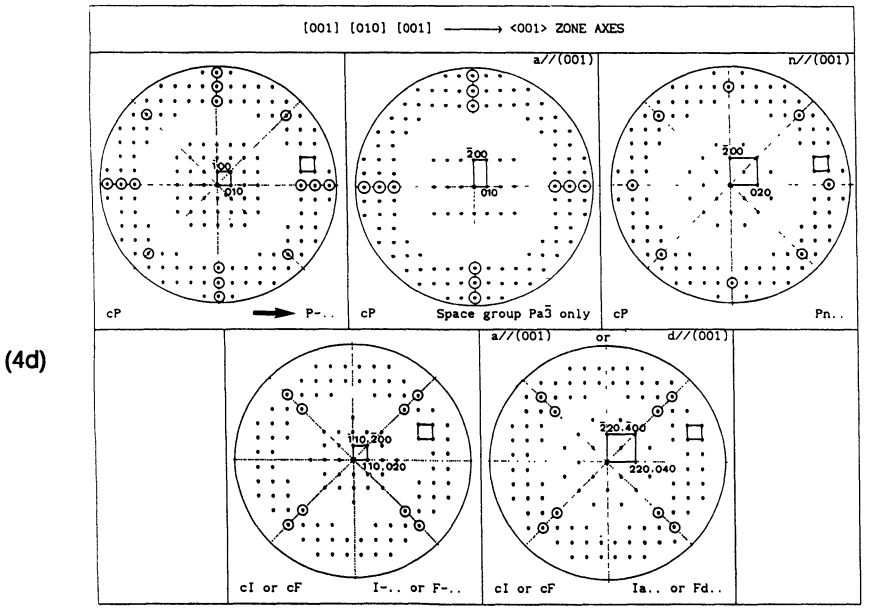

Fig. 4. — γ' Fe-N phase. a) b) c) < 100 > zone axis pattern. d) Theoretical < 100 > ZAPs for the cubic system. (Reproduced from Morniroli and Steeds, 1992, with permission of the publisher.)

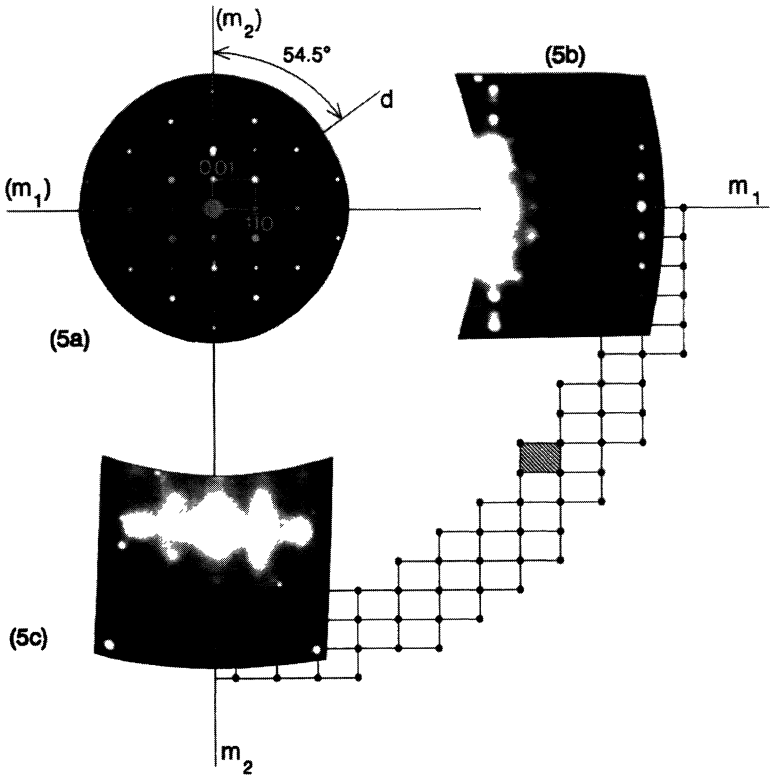

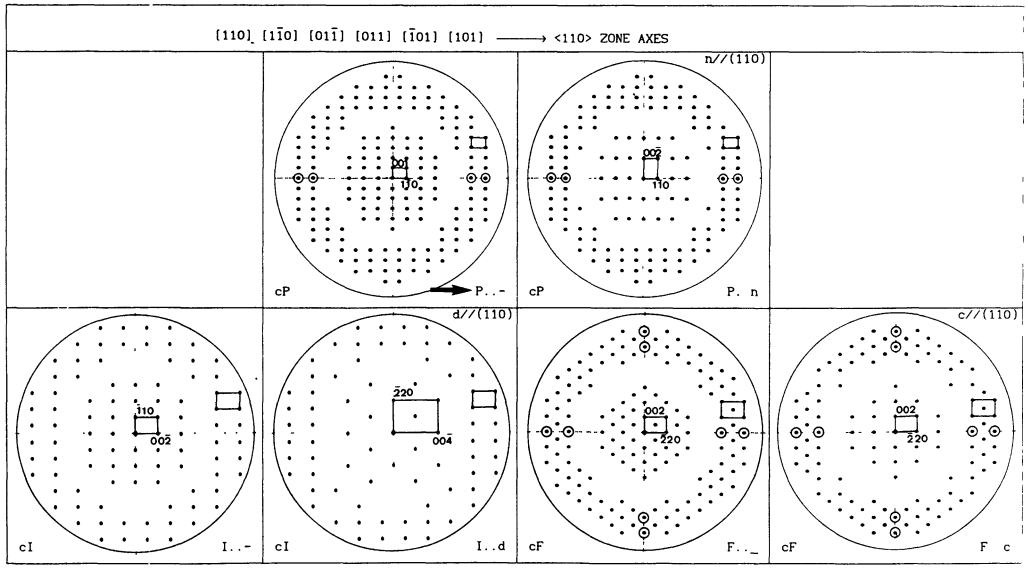

(5d)

Fig. 5. — γ' Fe-N phase. a) b) c) < 110 > zone axis pattern. d) Theoretical < 110 > ZAPs for the cubic system. (Reproduced from Morniroli and Steeds, 1992, with permission of the publisher.)

on mirrors m_1, m_2, and m_1', m_2'. According to the theoretical patterns given in figure 4d, the individual partial extinction symbol P-.. is inferred.

For the < 110 > ZAP (Figs. 5a, b, c), the rectangles drawn in the FOLZ and in the ZOLZ with their sides parallel to mirrors m_1, m_2, are non-centered and identical. FOLZ reflections are present on mirror m_1 but absent on mirror m_2. The individual partial extinction symbol P..- is deduced from comparisons with figure 5d.

By adding the two previous symbols, the partial extinction symbol P-.- is obtained. According to table 3.2 in reference [12], this is in agreement with nine space groups belonging to five point groups, as indicated in the following table:

point group	23	$m\bar{3}$	432	$\bar{4}3m$	$m\bar{3}m$
space group	P23 P2$_1$3	$Pm\bar{3}$	P432 P4$_2$32 P4$_1$32 P4$_3$32	$P\bar{4}3m$	$Pm\bar{3}m$

The Tanaka "multibeam" method is used to determine the point group. Since the possible point groups for the γ' phase are the same as those obtained for the γ phase in the previous case, the $< uuw >$ zone axes can be used once again.

We observed the [411] zone axis (Fig. 6a) because this pattern contains the superlattice reflections $(\bar{1}22, \bar{1}04)$ that are required for this analysis. The experimental pattern corresponds to the projected diffraction group $2mm1_R$ (Fig. 6b). This is in agreement with the point group $m\bar{3}m$. Hence, the space group for the γ' phase is $Pm\bar{3}\hat{m}$.

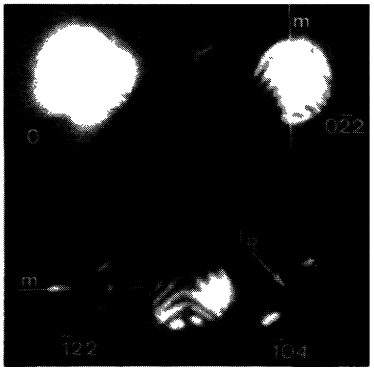

(6a)

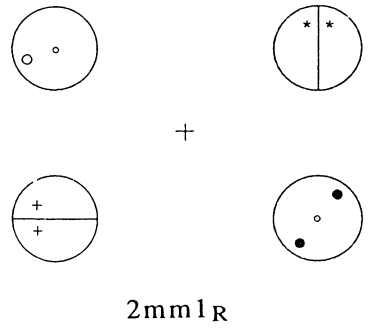

(6b)

Fig. 6. — γ' Fe-N phase. a) < 411 > zone axis Tanaka "multibeam" pattern. b) Symmetry elements for the $2mm1_R$ diffraction group.

The same conclusion can also be obtained from observation of the (4mm), 4mm "ideal" sym-

metry of the < 001 > ZAP (Figs. 4a, b, c). According to table IV, this symmetry corresponds to the point group $m\bar{3}m$ and then the space group is $Pm\bar{3}m$.

4.3 STUDY OF THE ε PHASE. — As in the case of the γ' phase, both fundamental and superlattice reflections are observed in microdiffraction patterns from the ε phase.

The highest "net" symmetries observed are (6 mm), 6 mm (Figs. 7a, b, c). According to tables I and II, the corresponding lattice is hexagonal, the zone axis is [0001] and the crystal system is either hexagonal or trigonal.

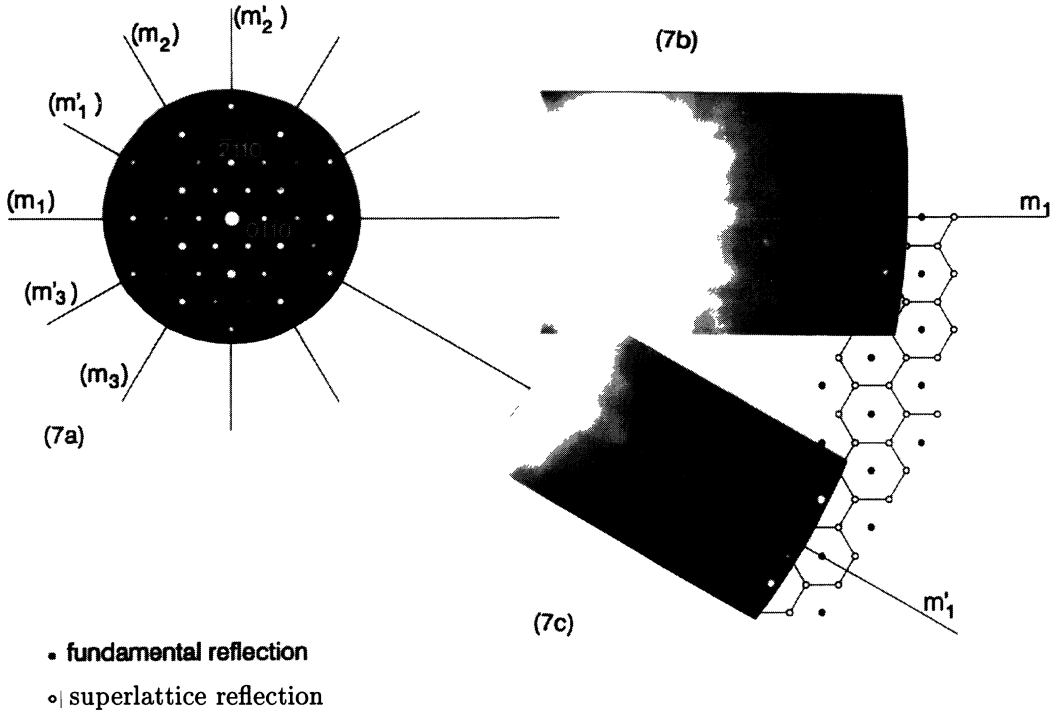

Fig. 7. — ε Fe-N phase. a) b) c) [0001] zone axis pattern.

For both hexagonal and trigonal crystal systems, the < $11\bar{2}0$ > and < $1\bar{1}00$ > zone axes must be observed in order to identify the possible glide planes (see Tab. III).

The < $11\bar{2}0$ > ZAP, given in figures 8a, b, c, does not display any periodicity difference between the ZOLZ and the FOLZ reflection nets, meaning that there is no glide plane perpendicular to the < $11\bar{2}0$ > direction. In addition, FOLZ reflections are only present on the mirror m_1. A direct comparison with figure 8d leads to the individual partial extinction symbol P.−. .

On the < $1\bar{1}00$ > ZAP (Fig. 9) the same rectangles with sides parallel to the mirrors m_1 and m_2 are observed in the ZOLZ and in the FOLZ. As a result, there is no glide plane perpendicular to the < $1\bar{1}00$ > direction. FOLZ reflections are present on mirror m_1, but absent on mirror m_2. The individual partial extinction symbol P..− is inferred from figure 9d.

From these two patterns, the partial extinction symbol P.−− is deduced. According to table 3.2

[12], this symbol is compatible with the following space groups:

		Point group						
	Extinction symbol	6	$\bar{6}$	6/m	622	6mm	$\bar{6}$2m $\bar{6}$m2	6/mmm
hexagonal system	P---	P6	P$\bar{6}$	P6/m	P622	P6mm	P$\bar{6}$2m P$\bar{6}$m2	P6/mmm
	P6$_3$--	P6$_3$		P6$_3$/m	P6$_3$22			
	P6$_2$--	P6$_2$ P6$_4$			P6$_2$22 P6$_4$22			
	P6$_1$--	P6$_1$ P6$_5$			P6$_1$22 P6$_5$22			

		Point group							
	Extinction symbol	3	$\bar{3}$	321	3m1	$\bar{3}$m1	312	31m	$\bar{3}$1m
trigonal system	P---	P3	P$\bar{3}$	P321	P3m1	P$\bar{3}$m1	P312	P31m	P$\bar{3}$1m
	P3$_1$--	P3$_1$ P3$_2$		P3$_1$21 P3$_2$21			P3$_1$12 P3$_2$12		

The specimen gives too poor a CBED pattern and it is not easy to determine the [0001] "ideal" symmetries from figure 7, so the identification of the point group is not possible. Nevertheless, we observe on both $< 1\bar{1}00 >$ and $< 11\bar{2}0 >$ ZAPs (Figs. 8a and 9a), that half of the reflections situated along the mirror m_2, i.e. the 000l reflections with l odd, are absent or very weak, meaning that these reflections are presumably kinematical forbidden reflections. Confirmation is obtained by tilting the specimen around the [0001]* reciprocal axis. The intensity of these reflections decreases and eventually vanishes. This proves the presence of a 6_3 screw axis parallel to the [0001] axis. The actual extinction symbol is then $P6_3 - -$ and the remaining possible space groups are reduced to $P6_3$, $P6_3/m$ or $P6_322$.

One notices that some $h\bar{h}0l$ reflections with l odd, for example the $03\bar{3}l$ reflections, seems to be absent on the $< 11\bar{2}0 >$ ZAP (Fig. 8a). Among the three possible space groups given above, only the $P6_322$ group exhibits reflection conditions for the $h\bar{h}0l$ reflections [12]. The space group of the ε phase is then $P6_322$.

5. Discussion.

The structures and space groups of the γ, γ' and ε phases reported from previous works are given in figures 10, 11 and 12 and in the following table:

phase	γ	γ'	ε
space groups	Fm$\bar{3}$m [13, 14]	Pm$\bar{3}$m [13, 15, 16] P$\bar{4}$3m [13]	P6$_3$22 [13, 17, 18] P312 [13, 17, 18] P$\bar{3}$1m [13, 14] P6$_3$/mmc [13, 14]

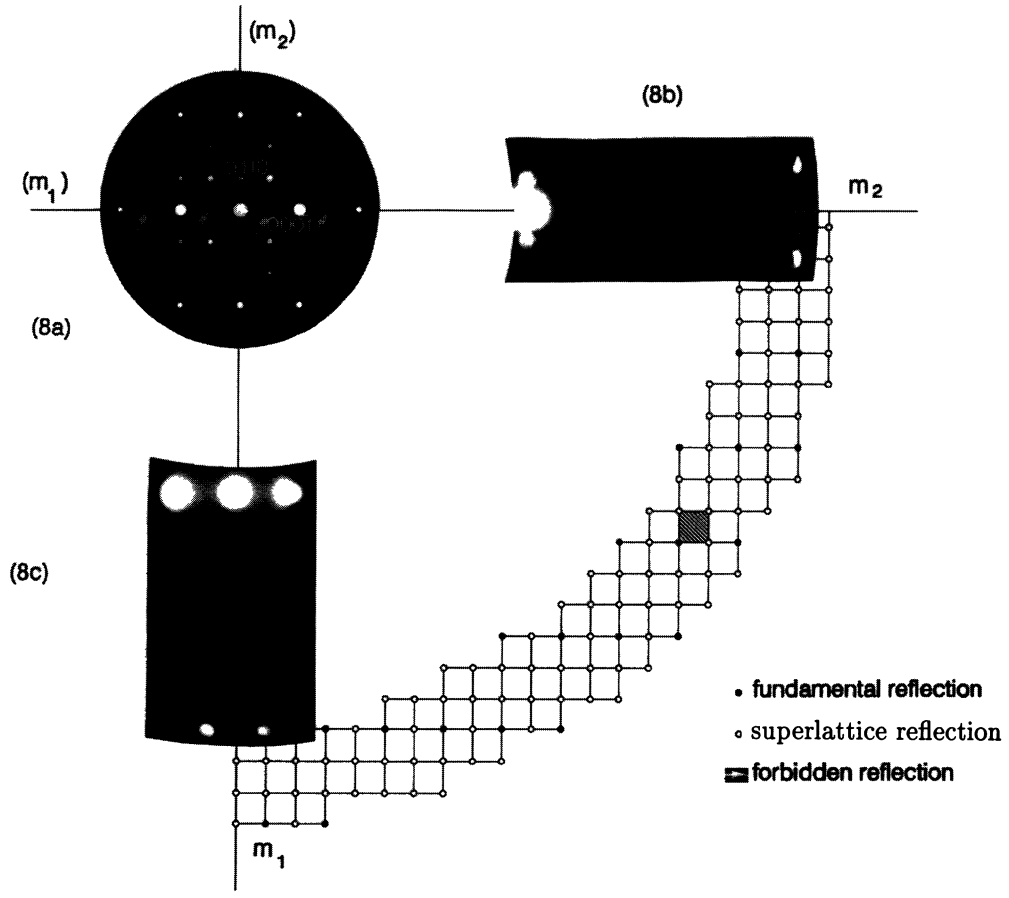

Fig. 8. — ε Fe-N phase. a) b) c) < 11$\bar{2}$0 > zone axis pattern. d) Theoretical < 11$\bar{2}$0 > ZAPs for the hexagonal lattice. (Reproduced from Morniroli and Steeds, 1992, with permission of the publisher.)

For the γ phase, the iron atoms adopt a fcc structure and the nitrogen atoms are located in octahedral interstices.

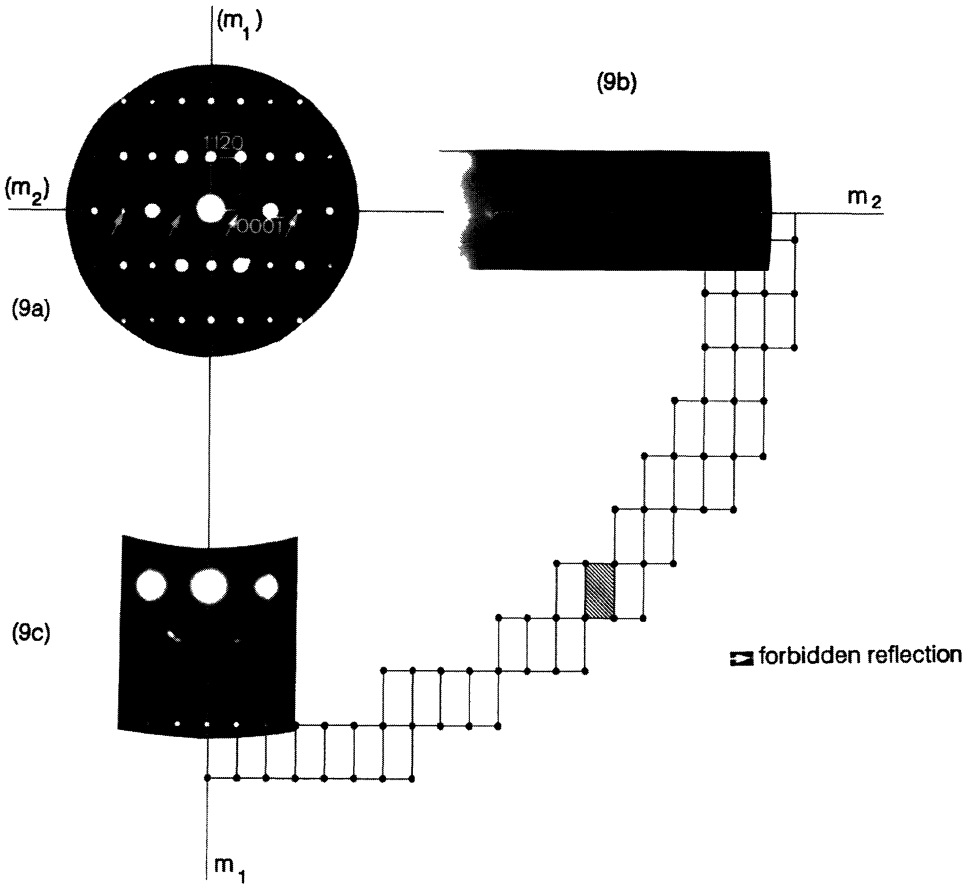

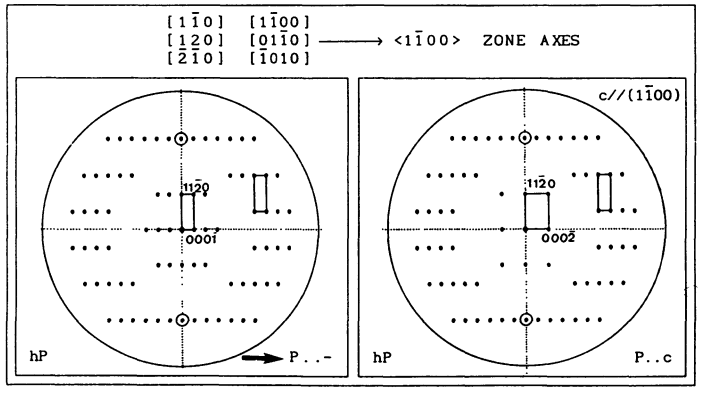

(9d)

Fig. 9. — ε Fe-N phase. a) b) c) < $1\bar{1}00$ > zone axis pattern. d) Theoretical < $1\bar{1}00$ > ZAPs for the hexagonal lattice. (Reproduced from Morniroli and Steeds, 1992, with permission of the publisher.)

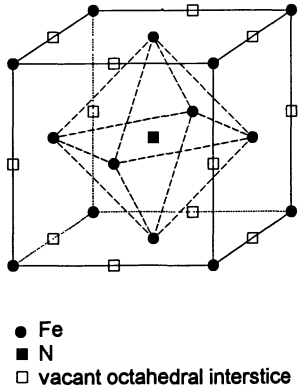

Fig. 10. — Description of the γ' structure.

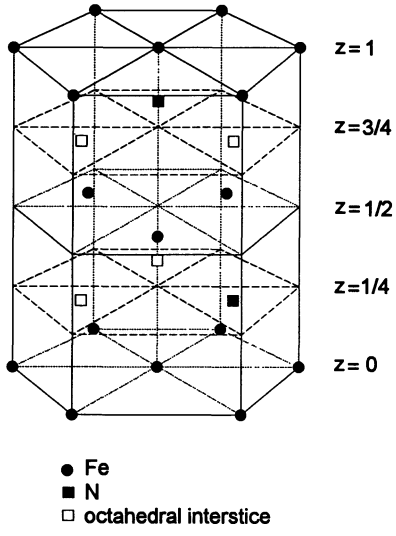

Fig. 11. — Description of the ε Fe-N (Fe_3N) structure.

For the γ' phase, only one octahedral interstice of this iron fcc structure is occupied by a nitrogen atom (Fig. 10).

For the ε phase, the iron atoms form a hexagonal close-packed structure. Hendricks and Kosting [18] propose that, depending on the nitrogen content, the nitrogen atoms are placed in an ordered manner in octahedral interstices. For Fe_2N, two thirds of the octahedral interstices are occupied in the layer at $z=1/4$ and one third is occupied in the layer at $z=3/4$ (Fig. 12). Two nitrogen atoms can never be in first neighbour position along the [0001] direction. The corresponding space group for this structure is P312.

For Fe_3N, one third of the octahedral interstices situated in the layer at $z=1/4$ and one third at $z=3/4$ are occupied by a nitrogen atom (Fig. 11). The eight octahedral interstices situated in first neighbour position (six in the same layer, one below and one above) around a filled interstice are empty. In that case the corresponding space group is $P6_322$.

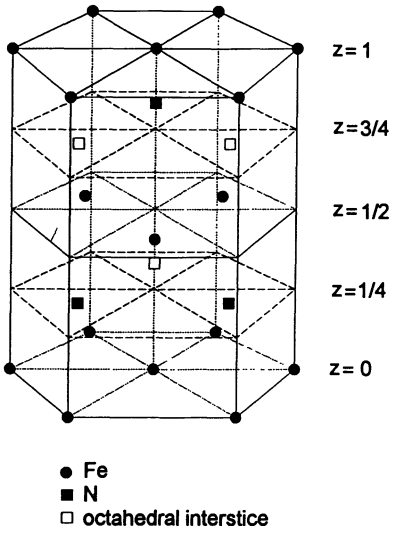

Fig. 12. — Description of the ε Fe-N (Fe_2N) structure.

The $P\bar{3}12/m$ and $P6_3/m\ 2/m\ 2/c$ space groups were also proposed by Wriedt, Gokcen and Nafziger [14].

If the nitrogen atoms are not ordered, then the space group is the same as that of the iron close-packed hexagonal lattice i.e. $P6_3/m\ 2/m\ 2/c$.

From our experimental results we have identified the $Fm\bar{3}m$ space group for the γ phase and the $Pm\bar{3}m$ space group for the γ' phase. Both results are in agreement with previous works [13-16].

For the ε phase, the $P6_322$ space group was identified. It is in agreement with the Fe_3N structure proposed by Hendricks and Kosting [18].

It is pointed out that, in order to identify these space groups, we have tried to follow as much as possible the formal scheme described in chapter 2. Nevertheless in some cases connected with strong texture or with poor quality CBED patterns, we were obliged to use other informations to reach the space group. This was the case for the cubic system of the γ and γ' phases which was not deduced according to the formal scheme but from observation of angles typical of the cubic system on $< 110 >$ ZAPs.

This was also the case with the ε phase whose space group was determined from identification of a 6_3 screw axis and from a careful analysis of $h\bar{h}0l$ forbidden reflections on $< 11\bar{2}0 >$ ZAPs.

6. Conclusions.

Microdiffraction patterns observed in connection with CBED patterns have allowed the identification of the space groups for the γ, γ' and ε phases of the iron-nitrogen phase diagram.

The method used for this analysis involves the following steps:

1) The crystal system and the zone axes are first identified from the ZOLZ and WP pattern "net" symmetries. Since it is imperative that the pattern (or the patterns) which displays the highest "net" symmetry is observed, care should be taken to ensure that the specimen does not exhibit preferential orientations which could prevent observation of the required "net" symmetry. If the highest "net" symmetry is not obtained experimentally, then information coming from other zone axes may be used to identify the crystal system conclusively (see the examples of the γ and γ' phases).

2) The Bravais lattice and the possible glide planes are respectively determined by observing the shift and the periodicity difference between the ZOLZ and the FOLZ reflection nets present on some typical zone axes. These two features are revealed clearly on the microdiffraction patterns and can be characterized by drawing the smallest rectangles (or squares) in the ZOLZ and the FOLZ and by observing the presence or the absence of FOLZ reflections along the "net" mirrors.

3) A partial extinction symbol is then simply deduced from comparisons with theoretical patterns, drawn for all possible cases. This leads to a few possible space groups.

These first three steps are usually easy to perform since only the positions of the reflections on the microdiffraction patterns are taken into account. Nevertheless it is important that the microdiffraction pattern contains 3D information i.e. that HOLZ reflections or at least FOLZ reflections are present on the microdiffraction pattern. If this is not the case, the specimen can be tilted along the "net" mirrors until more or less large sections of the FOLZ reflection net appear.

4) In order to remove the ambiguity between the possible space groups it is necessary to identify the point group. The Tanaka "multibeam" method and a method which involves observation of the "ideal" symmetry were used to do this. This stage in the identification process is more delicate to perform because it requires observation of the intensity of the reflections and therefore very accurate specimen orientation with respect to the electron beam.

Despite several experimental difficulties connected with:
- the texture , the small crystal size and the magnetism of the specimens,
- the absence of high order Laue zone reflections on most high symmetry zone axis patterns,
- the nitrogen atoms ordering,

it was possible to identify unambiguously the space groups of the three studied phases.

References

[1] BUXTON B.F., EADES J.A., STEEDS J.W. and RACKHAM G.M., *Proc. Roy. Soc.* (London) **A281** (1976) 171.
[2] TANAKA M., SAITO R. and SEKII H., *Acta Crystallogr.* **A39** (1983) 357.
[3] GJONNES J. and MOODIE A.F., *Acta Crystallogr.* **19** (1965) 65.
[4] MORNIROLI J.P. and STEEDS J.W., *Ultramicroscopy* **45** (1992) 219.
[5] STEEDS J.W. and EVANS N.S., in Proc. 38 th Annu. EMSA Meeting, San Francisco, 1980, Ed. G.W. Bailey, p. 188.
[6] RAGHAVAN M., YU KOO J. and PETKOVIC-LUTON R., *J. Metals* **35** (1984) 6.
[7] RAGHAVAN M., SCANLON J.C. and STEEDS J.W., *Met. Trans.* **15A** (1984) 1299.
[8] RAGHAVAN AYER M., KLEIN C.F. and ANGERS L., in Proc. 11th Int. Congr on Electron Microscopy, Kyoto (1986) p. 701.
[9] RAGHAVAN AYER M., *J. Electron Microsc. Tech.* **13** (1989) 16.
[10] STEEDS J.W. and VINCENT R., *J. Appl. Cryst.* **16** (1983) 317.
[11] BUERGER N.J., *Z. Kristallogr.* **91** (1935) 255.
[12] International Tables for Crystallography, Ed. T. Hahn (Reidel, Dordrecht, 1988).
[13] Binary alloy phase diagrams, Ed. T.B. Massalski, publ. American Society for metals (1990).
[14] WRIEDT H.A., GOKCEN N.A., NAFZIGER R.H., *Bull. alloy phase Diagrams* **8** (1987) 355.
[15] WYCKOFF R.W.G., Crystal Structures, Vol. 2, 2nd edition, (Interscience Publisher a division of John Wiley & Sons).
[16] MORNIROLI J.P., RICHARD O. and FOCT J., in: Proc. Coll. Franco-Ibérique de Microscopie Electronique, Barcelona (1991) p. 311.
[17] JACK K.H., *Acta Cryst.* **5** (1952) 404.
[18] HENDRICKS S.B. and KOSTING P.B., *Z. Krystallogr.* **74** (1930) 511.